Chemical surface diffusion coefficient and ordered $c(2 \times 2)$ adsorbate layer

1996 J. Phys.: Condens. Matter 8 1335

(http://iopscience.iop.org/0953-8984/8/10/006)

J. Phys.: Condens. Matter **8** (1996) 1335–1343. Printed in the UK

Chemical surface diffusion coefficient and ordered $c(2 \times 2)$ adsorbate layer

Pei-Lin Cao†‡, Min Qiu‡ and Lie-Quan Lee‡

† China Centre of Advanced Science and Technology (World Laboratory), PO Box 8730, Beijing 100080, People's Republic of China

‡ Department of Physics and State Key Laboratory of High Purity Silicon, Zhejiang University, Hangzhou 310027, People's Republic of China

Received 7 July 1995, in final form 20 November 1995

Abstract. Using the lattice gas model and transition-type-dependent type Monte Carlo method, we calculated the chemical surface diffusion coefficient with nearest-neighbour repulsion (ϵ_{nn}) and next-nearest-neighbour attraction (ϵ_{nnn}) ($\epsilon_{nn} = 2.0|\epsilon_{nnn}| = \epsilon_{int}$) directly from Fick's first law. Our results show that the chemical diffusion coefficient depends on the structure of the adsorbate layer. When $\epsilon_{int}/k_BT \geqslant 1.20$, the ordered lattice gas phase $c(2 \times 2)$ is established near $c = 0.50$. The presence of the ordered domains will greatly reduce the chemical surface diffusion coefficient.

1. Introduction

The diffusion of adsorbates on surfaces is one of the most important stages in many surface processes such as adsorption and desorption, film and crystal growth, and heterogeneous catalysis [1, 2]. A variety of experimental techniques are used to examine surface diffusion. Among these are field emission microscopy [3–5], field ionization microscopy (FIM) [6–8], laser-induced thermal desorption [9, 10] and, more recently, scanning tunnelling microscopy (STM) [11], and optical second-harmonic diffraction from a laser-induced monolayer grating [12]. Theoretical diffusion studies employ a wide variety of techniques, including transition state theory [13, 14], molecular dynamics computer simulation [15, 16], semiempirical quantum-chemical study [17] and the lattice gas (LG) model [18, 19]. The information from these experimental measurements and theoretical studies has already revealed some complicated mechanisms underlying the surface diffusion process. The surface diffusion is greatly affected not only by the structure and other physiochemical properties of the substrate but also by the structure of the adlayer itself and by the nature of the interaction of migrating species. As pointed out by Gomer [1], a number of questions for surface diffusion remain largely unanswered, perhaps the most puzzling is the relation of the surface diffusion coefficient to the phase structure of the adsorbate layer.

The LG model is applicable to many problems of surface diffusion. In general, it is too complicated for an exact mathematical solution of the master equation but rather easy to 'solve' it by Monte Carlo (MC) simulation, which requires a modest amount of computer resources. The information obtained from MC–LG modelling is enormously useful in providing some insight into the complicated mechanism of surface diffusion.

0953-8984/96/101335+09$19.50

In the MC–LG model, the self-diffusion coefficient D_i, which is also called the tracer diffusion coefficient, is calculated from the mean square displacement of a tracer particle at zero coverage in the usual way [20]:

$$D_i = \lim_{t\to\infty}(\langle r^2(t)\rangle/4t) \tag{1}$$

where $\langle r^2(t)\rangle$ is the mean square displacement of the ith particle at time t from its initial position at time 0. The response of an adsorbed layer to a gradient in chemical potential, most often simply a concentration (coverage) gradient, defines via Fick's law a chemical diffusion coefficient D (or sometimes called a collective diffusion coefficient). Except for FIM and STM, all the experiments mentioned above determine the chemical rather than the tracer diffusion coefficient. Because there are many interacting adatoms in the system, estimating D in the course of MC simulation of LGs is not as simple as estimating a tracer diffusion coefficient [21].

Up to now, only a very few results about the relation of the chemical diffusion coefficient to the order of the adsorbate layer have been presented. Recently using fluctuation and the Kubo–Green method, Uebing and Gomer [22] reported that, with the next-nearest-neighbour repulsive and nearest-neighbour attractive interactions between adparticles, at half-monolayer coverage, where the ordered $p(2\times 1)$ and $p(1\times 2)$ structures are completed, both diffusion coefficients (from fluctuation and the Kubo–Green method) increase by more than one order of magnitude. This result is similar to the reports in [19, 23], where much larger surface diffusion coefficients are shown in the vicinity of half-monolayer coverage.

Recently, using the time-dependent MC method [24] to overcome the 'rare-event problem', we proposed a new calculation method of the real time in MC simulation and developed a special technique of computation to move rapidly towards faster convergence [25]; then the algorithm is so efficient that the computational difficulties due to 'noise' inherent in the data mentioned above have been overcome. These developments enable us to calculate the chemical diffusion coefficient directly from Fick's law. For simplicity we called this method the transition-type-dependent Monte Carlo (TTDMC) method. If there are interactions between adparticles, the ordered structure may be completed in some region of the adsorbate layer; then we can study the relation of the chemical diffusion coefficient to the order of adsorbate layer in a more direct way. In this paper, repulsive nearest-neighbour and attractive next-nearest-neighbour interactions are used, then the $c(2\times 2)$ structure may be present near the half-monolayer region.

2. Method

The TTDMC [25] simulation, based on a LG model, was performed for a two-dimensional square lattice, with periodic-boundary conditions in one direction (say y) and with a stationary concentration gradient in the other direction (say x). $L_x \times L_y$ with $L_x = 72$ and $L_y = 30$ were used in these calculations. The coverage in the first four columns of $L_x = 1, 2, 3$ and 4 is fixed at c_0 and in the last column of $L_x = 72$, the coverage is fixed at zero by adding or subtracting particles in the process of diffusion. By setting some initial adparticle concentration gradients (e.g. linear gradients), a stationary gradient is assumed to be established if the total number of adparticles in the system and the adparticle current of diffusion start to fluctuate about mean values. In our calculations, a total of 4×10^6 hops of particles are generally taken to ensure this condition.

The binding energy of a typical adparticle to the surface is given by

$$\epsilon_{ij} = \epsilon_b^0 - I\epsilon_{nn} - J\epsilon_{nnn} \tag{2}$$

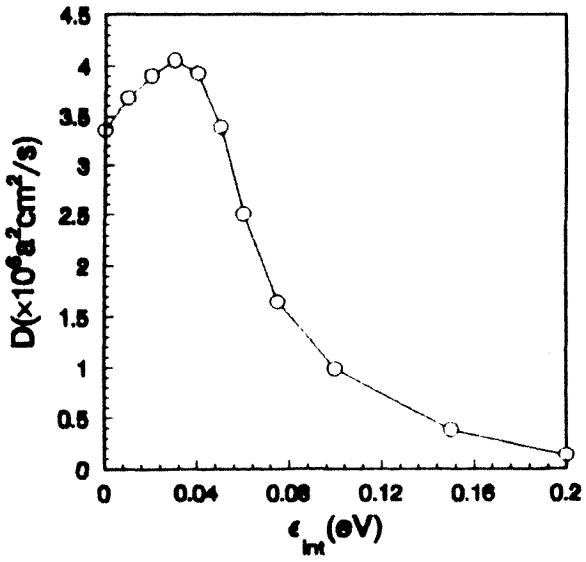

Figure 1. Average chemical diffusion coefficients $\bar{D}$ versus ϵ_{int}.

where I and J are the number of nearest- and next-nearest-neighbour adparticles, and ϵ_{nn} and ϵ_{nnn} are the nearest- and next-nearest-neighbour interaction energies, respectively. The binding energy of an isolated adatom to the substrate is given by ϵ_b^0. The activation barrier, which is calculated from the intersection point between harmonic potential wells centred on adjacent sites, is defined as [24]

$$\epsilon_{ij,kl} = \epsilon_m^0 + (\epsilon_{ij} - \epsilon_{kl})/2 + (\epsilon_{ij} - \epsilon_{kl})^2/16\epsilon_m^0 \tag{3}$$

where (i, j) and (k, l) refer to the initial and final site, the migration barrier for an isolated adparticle is given by ϵ_m^0. In our LG model, migration is allowed only to vacant nearest-neighbour sites [26].

The average concentration on the L_xth column is given by

$$\bar{C}(L_x) = \left(\sum_i n_{L_x} \tau_i \Big/ \sum_i \tau_i \right) \left(\frac{1}{30a^2} \right) \tag{4}$$

where τ_i is the real time interval of the ith TTDMC cycle, n_{L_x} is the number of adparticles in the L_xth column at that time, and a is the nearest-neighbour distance. In our calculations, summation began after the stationary concentration gradients were established after about 4×10^6 hops of adparticles. The particle currents are obtained by the total particles entering the column of $L_x = 72$ divided by the total real time interval Δt and $30a$. Δt is calculated by [25]

$$\begin{aligned} \Delta t &= \sum \tau_i = \sum \frac{\tau_i^0}{M} \\ \tau_i^0 &= \frac{1}{\nu} \exp\left(\frac{\epsilon_{bi}}{k_B T} \right) \end{aligned} \tag{5}$$

where M is the total number of possible transition types, ϵ_{bi} is the energy barrier for the ith transition type and Σ represent the sum over all jumps. Generally speaking, a smooth average concentration curve (versus L_x) will be obtained after 4×10^7 TTDMC cycles;

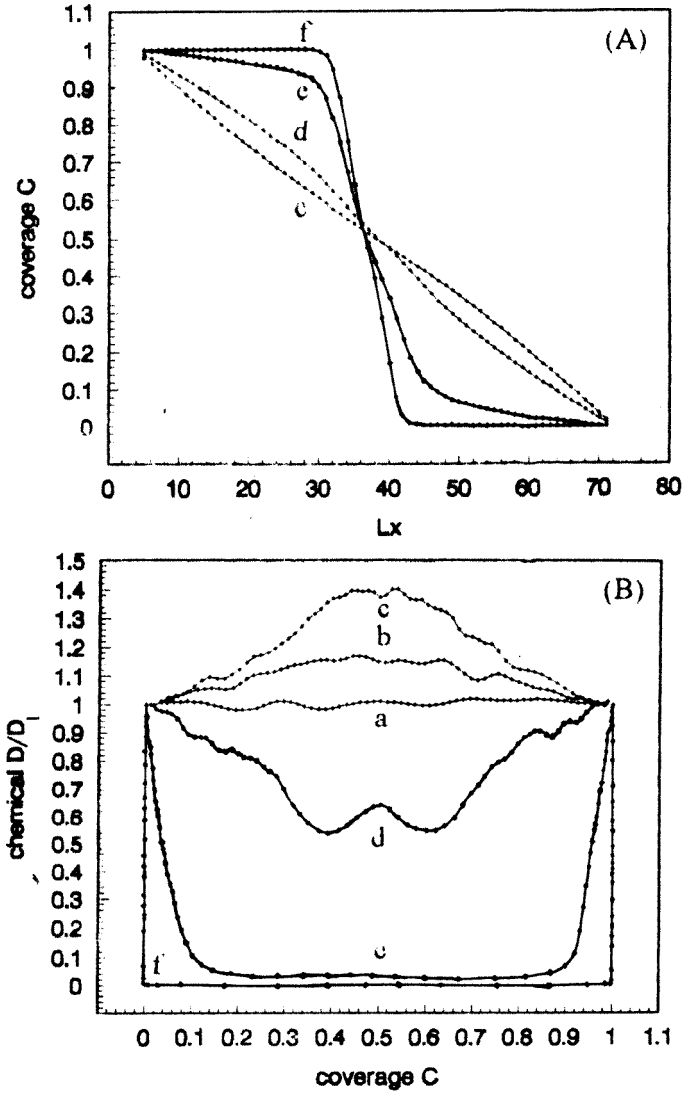

Figure 2. (A) Concentration C versus x and (B) chemical diffusion coefficient D/D_1 versus concentration C ($k_BT = 0.05$ eV): curves a, $\epsilon_{int} = 0.00$ eV; curves b, $\epsilon_{int} = 0.01$ eV; curves c, $\epsilon_{int} = 0.03$ eV; curves d, $\epsilon_{int} = 0.06$ eV; curves e, $\epsilon_{int} = 0.15$ eV; curves f, $\epsilon_{int} = 0.40$ eV.

it will take about 24 CPU h on our 486 computer. Then D is obtained from the particle current divided by the negative concentration gradient:

$$D = -\frac{J}{\mathrm{d}C/\mathrm{d}x} = -\frac{N}{(\mathrm{d}\bar{C}/\mathrm{d}x)s\Delta t} \tag{6}$$

where N is the total number of particles across the plane with area s (perpendicular to x) in the time interval Δt, and $\bar{C}$ is the average concentration calculated using equation (4). The advantage of this technique is that, from the profile of the particle concentration, not only the average but also D as functions of concentration (or coverage) are obtained.

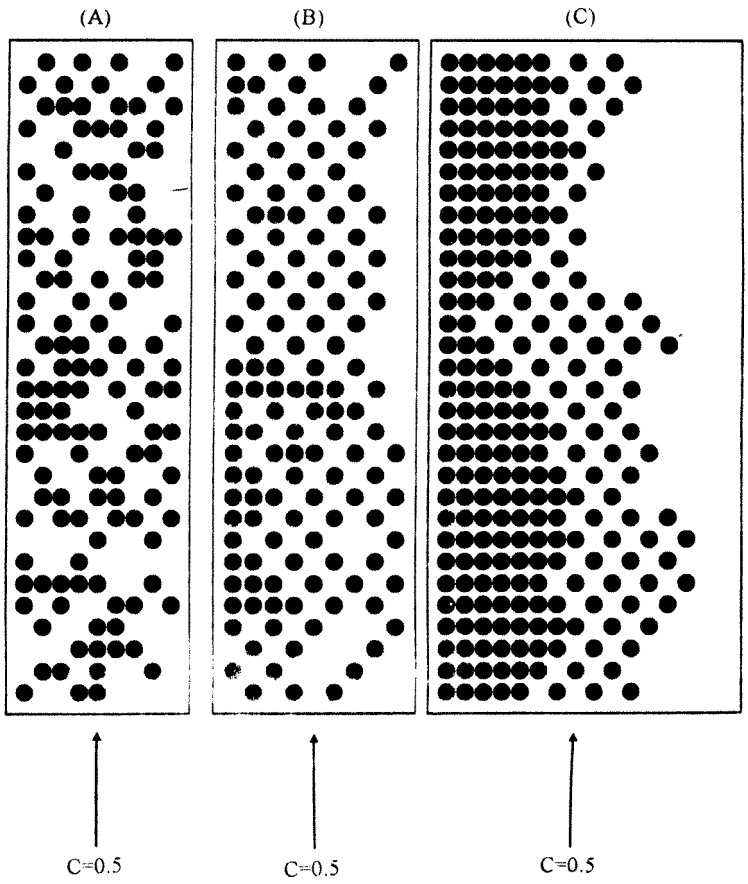

Figure 3. 'Snapshots' of representative equilibrium distribution of diffusing adparticles near $c = 0.50$ for (A) $\epsilon_{int} = 0.03$ eV ($\epsilon_{int}/k_BT = 0.60$), (B) $\epsilon_{int} = 0.15$ eV ($\epsilon_{int}/k_BT = 3.0$) and (C) $\epsilon_{int} = 0.40$ eV ($\epsilon_{int}/k_BT = 8.0$).

3. Results and discussion

It is well known that, if there are nearest-neighbour repulsive and next-nearest-neighbour attractive interactions between adparticles (the strength of the interaction denoted by ϵ_{nn} and ϵ_{nnn}), the $c(2 \times 2)$ ordered structure may be established in an adsorbate layer. In our calculations we assume that $\epsilon_{nn} = 2.0|\epsilon_{nnn}| = \epsilon_{int}$. As a first step, we calculated the chemical diffusion coefficients with different ϵ_{int}. The results of average diffusion coefficients $\bar{D}$, calculated using (6) in which the average gradient from $L_x = 4$–72 is used, are shown in figure 1. In these calculations, the parameters are $c_0 = 1.0$, $k_BT = 0.05$ eV, $\epsilon_b^0 = 2.0$ eV ($40\ k_BT$), $\epsilon_m^0 = 0.40$ eV and $\nu = 10^{10}$ s^{-1}. The calculated results show that, as the interaction energy ϵ_{int} increases, $\bar{D}$ first increases, and then decreases. As ϵ_{int} approaches about $0.75\ k_BT$, the $\bar{D}$ reaches its maximum value. As discussed in Naumovets and Vedula [2], in the presence of lateral interactions, an additional driving force of diffusion acts together with the concentration gradient; the lateral attraction will reduced the surface diffusion, and the lateral repulsion will increase the surface diffusion. In these calculations, the strength of nearest-neighbour repulsion is larger than that of next-nearest-neighbour

attraction; it is easy to understand why the chemical surface diffusion will increase with increasing ϵ_{int}. However, as shown in figure 1, when $\epsilon_{int}/k_BT > 1.0$, $\bar{D}$ will decrease with increase in the strength of lateral interaction ϵ_{int}. We shall discuss this in more detail below.

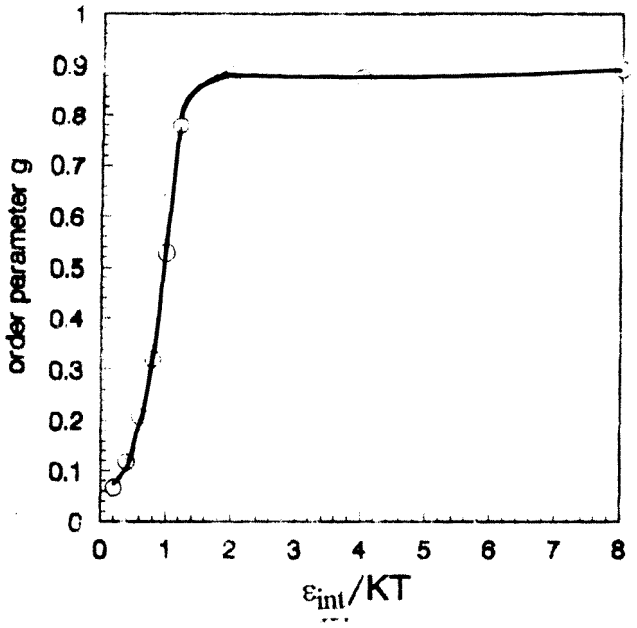

Figure 4. Relation between the order parameter g near $C = 0.5$ and ϵ_{int}/k_BT ($k_BT = 0.05$ eV).

Other important data obtained from the calculations are the chemical diffusion coefficient as a function of concentration (or coverage). Our results for the Langmuir LG, i.e. no lateral interaction, show that the concentration against x is perfectly linear with x; so the concentration gradient is constant. As expected, the diffusion coefficient D is independent of concentration. Figure 2(A) shows the calculated concentration versus x, and figure 2(B) the chemical diffusion coefficient as a function of concentration (coverage here), with the interaction strengths $\epsilon_{int} = 0.00$ eV (curve a), 0.01 eV, (curve b), 0.03 eV (curve c), 0.06 eV (curve d), 0.15 eV (curve e), and 0.40 eV (curve f). $k_BT = 0.05$ eV. Because the concentration curves are too close each other, in figure 2(A), only $\varepsilon_{int} = 0.03$ eV (curve c), 0.06 eV (curve d), 0.15 (curve e) and 0.40 eV (curve f) are shown. The parameters are the same as above. Figure 2(B) shows that the chemical diffusion exhibits strong non-monotonic behaviour as a function of concentration. Near $c = 0.5$, the chemical diffusion coefficient may be a maximum or minimum. In the case of $\epsilon_{int} = 0.03$ eV (0.6 k_BT), as the concentration increases from 0.0 to 1.0, the chemical diffusion coefficient is increased from D_1, a low coverage limit, to its maximum value at about $c = 0.50$ and then decreases to D_1 at $c = 1.0$. The maximum value of D for $\epsilon_{int} = 0.03$ eV is larger than that of $\epsilon_{int} = 0.01$ eV. When ϵ_{int} is increased from 0.03 to 0.06, 0.15 and 0.40 eV, the chemical diffusion coefficient near $c = 0.50$ is greatly decreased, and this reduces the average chemical diffusion coefficient, as indicated above in figure 1. Figures 3(A), 3(B) and 3(C) show 'snapshots' of representative equilibrium distribution of diffusing adparticles for $\epsilon_{\rm int} = 0.03$ eV ($\epsilon_{int}/k_BT = 0.6$), $\epsilon_{\rm int} = 0.15$ eV ($\epsilon_{int}/k_BT = 3.0$) and $\epsilon_{\rm int} = 0.40$ eV

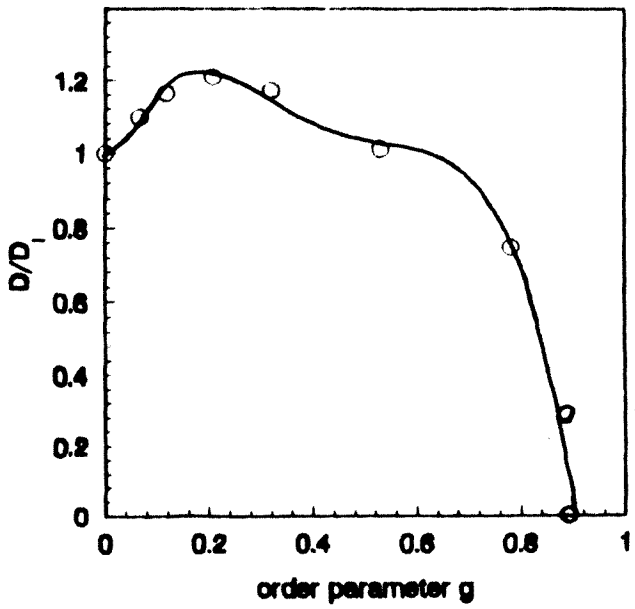

Figure 5. Calculated chemical diffusion coefficients D/D_1 near $C = 0.50$ as a function of the order parameter g.

($\epsilon_{int}/k_BT = 8.0$), respectively. Clearly an almost perfect $c(2 \times 2)$ structure is observed in the region near $c = 1/2$ for $\epsilon_{int}/k_BT = 3.0$ and 8.0 but, for $\epsilon_{int}/k_BT = 0.6$, this perfect structure does not appear. For a perfect $c(2\times2)$ structure, we know that its coverage is 0.50, and there is not any nearest-neighbour atom. If there is complete disorder, for $c = 0.50$, the average nearest-neighbour atom number is 2.0; so we define an order parameter g for $c(2 \times 2)$:

$$g = \frac{|2 - n_{av}|}{2} \tag{7}$$

where n_{av} is the average nearest-neighbour atom number, g stands for the perfection of the $c(2 \times 2)$ structure. Figure 4 shows the relation between calculated g near $C = 0.5$ and ϵ_{int}/k_BT. When ϵ_{int}/k_BT increases from 0 to near 1.20, g increases quite rapidly, and the ordered structure is almost complete at about $\epsilon_{int}/k_BT \geqslant 1.20$. Uebing [27] pointed out that, with the nearest-neighbour repulsive interaction, a $c(2 \times 2)$ ordered LG phase in the range $0.4 \leqslant c \leqslant 0.6$ exists below T_c with $\epsilon_{nn}/k_BT_c = 2|\ln(\sqrt{2} - 1)| = 1.76$. In our calculations, both the nearest-neighbour repulsion and the next-nearest-neighbour attraction are agents of the ordered structure; it is reasonable to think that the strength ϵ_{agn} of the agent is equal to ϵ_{nn} in [27], but in our calculations $\epsilon_{agn} = \epsilon_{nn} + |\epsilon_{nnn}| = 1.50\epsilon_{int}$. Our result in figure 4 is in good agreement with that in [27]. The calculated chemical diffusion coefficient D/D_1 for $c = 0.50$ as a function of order parameter g is shown in figure 5. For $g \leqslant 0.30$, it is reasonable to think that the $c(2 \times 2)$ ordered structure has not formed yet and, because of the increasing nearest-neighbour repulsive interaction, the chemical diffusion coefficient is increasing and is larger than D_1. However, as shown in figure 5, the chemical diffusion coefficient will be greatly decreased for $g > 0.6$, especially as g approaches 1.0, i.e. the perfect $c(2\times2)$ ordered structure. It is worthwhile to note that in figure 4, even if ϵ_{int}/k_BT

is as large as 8.0, the order parameter g does not approach 1.0 but is still equal to about 0.9 in our system. In order to understand this problem, let us consider curve f in figure 2 and figure 3(C). It is clear that, in the case when $\epsilon_{int}/k_BT = 8.0$, the concentration gradient is very large near $c = 0.50$, the narrow ordered $c(2 \times 2)$ domain is a region very highly resistant to diffusion, and the average chemical diffusion coefficient is very small now (the calculated value is 0.9342×10^4 a^2 cm^2 s^{-1}, compared with $D_1 = 0.3355 \times 10^7$ a^2 cm^2 s^{-1}), because the concentration gradient near $c = 0.50$ is so large that it is impossible to form a perfect $c(2 \times 2)$ domain there.

Now we discuss the relation between the average chemical diffusion coefficient and k_BT with $\epsilon_{int} = 0.05$ eV (curve a), 0.10 eV (curve b), and 0.20 eV (curve c). Our calculated results are shown in figure 6. It is obvious that, as $k_BT \approx 1.50\epsilon_{int} = \epsilon_{agn}$ $(= k_BT_m)$, $\bar{D}/D_1$ reaches its maximal value. A decrease in T from T_m will decrease $\bar{D}/D_1$ because of the formation of the ordered structure; an increase in T from T_m will decrease $\bar{D}/D_1$, too. As expected, when T is very high and k_BT/ϵ_{agn} is much larger than 1.0, the influence of the interaction will be negligible, and $\bar{D}/D_1$ will approach 1.0.

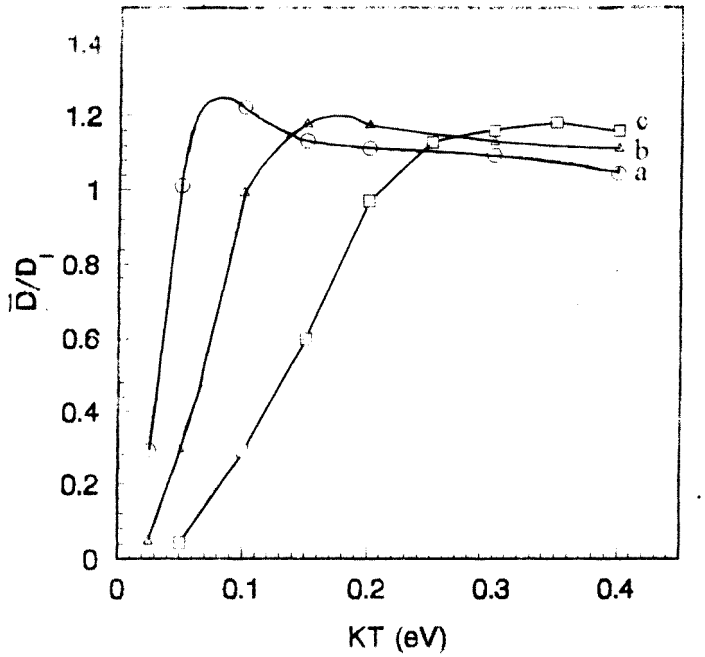

Figure 6. The average chemical diffusion coefficient $\bar{D}/D_1$ versus k_BT (eV): curve (a) $\epsilon_{int} = 0.05$ eV; curve (b) $\epsilon_{int} = 0.10$ eV; curve (c) $\epsilon_{int} = 0.15$ eV.

Finally, we compare our calculated results with those in [19, 22]. As mentioned above, the results in [19, 22] show much higher surface diffusion coefficients in the vicinity of half-monolayer coverage. More detailed relations of D to the order parameter g and of g to ϵ_{int}/k_BT are obtained in this work. As g is small, under the action of the nearest-neighbour repulsion, D increases with increase in ϵ_{int}/k_BT. However, as g becomes close to 1.0, i.e. to the perfect ordered structure, the chemical surface diffusion coefficients greatly decrease. Although there was no order parameter result in [19], from the ϵ_{int}/k_BT-value in that paper, it is reasonable to think that an almost perfect $c(2 \times 2)$ structure is established close to the

half-monolayer region in their models. The reasons for these discrepancies are not very clear now. In addition, the experimental results on the relation of D to the phase structure of adsorbate, e.g. as cited in [1, 23], show very complicated features. All these facts mean that, in order to obtain deeper insight into this relation, more experimental and theoretical studies have to be done. It is probable that these questions could be resolved at least in part by MC modelling, although it is not clear how elucidating the results will be [1].

4. Summary

The present work shows that the chemical diffusion coefficient depends on the structure of the adsorbate layer. When $\epsilon_{int}/k_BT > 1.2$ ($\epsilon_{agn}/k_BT > 1.8$), the ordered LG phase $c(2 \times 2)$ is established near $c = 0.50$. The presence of the ordered domain will greatly reduce the chemical surface diffusion coefficient.

Acknowledgment

This work was supported by the National Science Foundation of China.

References

[1] Gomer R 1990 *Rep. Prog. Phys.* **53** 917
[2] Naumovets A G and Vedula Yu S 1985 *Surf. Sci. Rep.* **4** 365
[3] Muller E W 1953 *Ergeb. Exakten Naturwiss* **27** 290
[4] Gomer R 1973 *Structure and Properties of Metal Surfaces (Honda Memorial Series on Material Science)* (Tokyo: Maruzen) pp 128–63 (R)
[5] Blaszczyszyn M *et al* 1983 *Surf. Sci.* **131** 433
[6] Kellogg G L 1985 *J. Chem. Phys.* **83** 852
[7] Binnig G, Fuchs H and Stoll E 1986 *Surf. Sci.* **169** L295
[8] Ehrlich G 1991 *Surf. Sci.* **246** 1
[9] Arena M V, Westre E D and George S M 1993 *Surf. Sci.* **261** 129
[10] Meixner D L and George S M 1993 *Surf. Sci.* **297** 27
[11] Wen J-M, Chang S-L, Burnett J W, Evans J W and Thiel P A 1994 *Phys. Rev. Lett.* **73** 2591
[12] Xiao Xu-Dong, Zhu X D, Daum W and Shen Y R 1991 *Phys. Rev. Lett.* **66** 2352; 1992 *Phys. Rev.* B **46** 9732
[13] Doll J D and McDowell H K 1982 *J. Chem. Phys.* **77** 479
[14] Landerdale J G and Truhlar D G 1985 *Surf. Sci.* **164** 558
[15] DeLorenzi G and Jacucci G 1982 *Surf. Sci.* **116** 391
[16] Voter A F and Doll J D 1985 *J. Chem. Phys.* **82** 80
[17] Cao P L and Zhang Z G 1989 *Phys. Rev.* B **39** 9963
[18] Hill T H 1956 *Statistical Mechanics* (New York: McGraw-Hill) p 302
[19] Bowker M and King D A 1978 *Surf. Sci.* **71** 583; **72** 208
[20] Mak C H, Anderson H C and George S M 1988 *J. Chem. Phys.* **88** 4052
[21] Kehr K W and Binder K 1983 Simulation of diffusion in lattice gases and related kinetic phenomena *Application of the Monte Carlo Methods in Statistical Physics (Top. Curr. Phys. 36)* K Binder (Berlin: Springer)
[22] Uebing C and Gomer R 1994 *J. Chem. Phys.* **100** 7759
[23] Reed D A and Ehrlich G 1981 *Surf. Sci.* **102** 588
[24] Bowler A M and Hood E S 1991 *J. Chem. Phys.* **94** 5162
[25] Cao P L 1994 *Phys. Rev. Lett.* **73** 2595
[26] Ehrlich G 1982 *CRC Crit. Rev. Solid State Mater. Sci.* **10** 391
[27] Uebing C 1994 *Phys. Rev.* B **49** 13 913